Spin waves and magnetic anisotropy in ultrathin (111)-oriented cubic films

1998 J. Phys.: Condens. Matter 10 2171

(http://iopscience.iop.org/0953-8984/10/9/019)

J. Phys.: Condens. Matter **10** (1998) 2171–2180. Printed in the UK PII: S0953-8984(98)88776-6

Spin waves and magnetic anisotropy in ultrathin (111)-oriented cubic films

G Gubbiotti†‡, G Carlotti‡§ and B Hillebrands‡

† Unità INFM, Dipartimento di Fisica dell'Università, Via Pascoli, 06100 Perugia, Italy
‡ Universität Kaiserslautern, Erwin-Schrödinger-Strasse 56, 67663 Kaiserslautern, Germany

Received 28 October 1997

Abstract. The dispersions of dipolar (Damon–Eshbach modes) and exchange-dominated spin waves are calculated for in-plane-magnetized thin and ultrathin cubic films with (111) crystal orientation and the results are compared with those obtained for the other principal planes. The properties of these magnetic excitations are examined from the point of view of Brillouin light scattering experiments. Attention is paid to the study of the spin-wave frequency variation as a function of the magnetization direction in the film plane for different film thicknesses. Interface anisotropies and the bulk magnetocrystalline anisotropy are considered in the calculation. A quantitative comparison between an analytical expression obtained in the limit of small film thickness and wave vector and the full numerical calculation is given.

1. Introduction

The study of spin waves in magnetic films with cubic symmetry has proved to be very useful for determining magnetic anisotropy constants. Most previous studies, however, have only considered (100)- and (110)-oriented films [1–8]. For the (111) orientation, spin-wave frequency calculations have not been presented so far, probably due to the more complicated algebra involved and due to the lack of experimental data. Recently, an appreciable directional in-plane dependence of the spin-wave frequency has been observed by means of ferromagnetic resonance (FMR) in thin Fe(111) films and Fe(111)/Cu(111) multilayers [9] as well as by means of Brillouin light scattering [10] (BLS) in ultrathin Ni films. This latter technique, which is based on the inelastic scattering of photons by thermally excited spin waves (thermal magnons), has proved to be a very powerful tool for investigating magnetic properties in magnetic films and multilayers through the detection of spin waves with non-zero wave vector. From BLS measurements of the spin-wave frequencies as a function of the direction and magnitude of the in-plane wave vector, $q_{\parallel}$, and the direction and strength of the externally applied field, magnetic parameters such as the in-plane anisotropy constants can be determined. The capability of BLS for determining the interface anisotropy constants is particularly relevant for the (111) plane of a cubic crystal. This is because torque measurements, like BLS ones, are always more sensitive to high-order anisotropies, such as the sixfold one in the (111) orientation, than static methods, which yield at best a very weak directional dependence of the free energy on the (111) plane,

§ Author to whom any correspondence should be addressed: Dr Giovanni Carlotti, Università di Perugia, Dipartimento di Fisica, Via A Pascoli, 06100 Perugia, Italy; e-mail: carlotti@pg.infn.it; telephone: +39 75 585 3067; fax: +39 75 44666.

0953-8984/98/092171+10$19.50

since, for an in-plane-magnetized film, the first-order magnetocrystalline anisotropy gives an isotropic contribution [11].

The aim of this paper is to fill the gap existing in the literature concerning the characteristics of the spin-wave spectrum of thin and ultrathin magnetic films with (111) orientation. The very new experimental results obtained by means of BLS [10], which show an appreciable in-plane directional dependence of the spin-wave frequency on the Ni(111) plane, and the necessity of interpreting them in terms of the anisotropy constants have motivated the theoretical study that we present here. The spin-wave frequency is calculated in the dipole-exchange regime assuming an in-plane-magnetized Ni film and including both interface and bulk anisotropy. This permits us to obtain the frequency dispersion as a function of both the film thickness and the direction of propagation on the surface plane.

2. The calculation procedure

In order to calculate the spin-wave frequency in the case of an in-plane-magnetized (111)-oriented cubic film, we make reference to a continuum model previously developed by one of us for (100)- and (110)-oriented films, and we use the same type of nomenclature [1]. The geometry is defined such that the x-axis is normal to the film interfaces at $x = 0$ (upper interface) and $x = -L$ (lower interface), while the applied field is taken along the z-axis. The film is considered to be infinite in the plane and the spin-wave propagation is assumed to be perpendicular to the applied field with a wave vector $q_{\parallel}$ defined by the light scattering geometry. The calculation relies upon resolving the equation of motion (the linearized Landau–Lifshitz torque equation and the magnetostatic Maxwell equations) for the magnetic layer with appropriate boundary conditions. Inclusion of terms resulting from exchange interaction yields six solutions for the dynamic components of the fields, which are classified according to the wave-vector components perpendicular to the layer ($q_{xi}, i = 1, 2, \ldots, 6$) [1]. From the magnetic and Rado–Weertman boundary conditions at the film interfaces, a system of eight linear homogeneous equations in the fluctuating fields inside (h_{xi}) and outside the layer (h^e_{x1} and h^e_{x2}) is obtained. The problem of finding solutions for the propagating spin waves is therefore reduced to that of finding the zeros of the 8×8 boundary condition determinant. A computer program has been written to search for the frequencies that correspond to the roots of this determinant. Although this is a standard and well established procedure, it should be noted that the calculations are a little bit more complicated when the (111) crystal orientation is considered, because of the additional contributions in the secular equation given by the magnetocrystalline and interface anisotropy fields H_{γ} and $H_{\gamma'}$ (see below), which are zero in the (100) and (110) orientations.

In the following we distinguish between volume and interface anisotropy contributions. The former contains the magnetocrystalline anisotropy which originates from the coupling of the magnetization to the crystallographic symmetry, while the latter is due to the lack of translational symmetry along the film normal. These anisotropy fields shift the magnetic excitation frequency. We point out that in this paper we only consider cubic anisotropy, while the possible presence of non-cubic terms, such as uniaxial in-plane anisotropy of magnetoelastic origin, is not taken into account.

For cubic crystals and referring to a Cartesian coordinate system aligned with the principal crystallographic axes, the free energy associated with the volume anisotropy, E_{ani}, is defined as

$$E_{ani} = K_1(\alpha_x^2\alpha_y^2 + \alpha_x^2\alpha_z^2 + \alpha_y^2\alpha_z^2) \tag{1}$$

where the α_i, $i = x, y, z$, are the direction cosines of the magnetization relative to the crystallographic axes and K_1 is the first non-vanishing-order magnetocrystalline anisotropy constant for a cubic system. If spherical coordinates are introduced, the explicit forms for E_{ani} relative to the three principal crystal orientations are [1, 12]

(100) $$E_{ani} = K_1(\cos^2\theta\sin^2\theta + \sin^4\theta\cos^2\phi\sin^2\phi) \tag{2}$$

(110) $$E_{ani} = \frac{K_1}{4}\left\{\cos^4\theta + \sin^4\theta[\sin^4\phi + \sin^2(2\phi)] + \sin^2(2\theta)\left[\cos^2\phi - \frac{1}{2}\sin^2\phi\right]\right\} \tag{3}$$

(111) $$E_{ani} = K_1\left\{\frac{1}{3}\cos^4\theta + \frac{1}{4}\sin^4\theta - \frac{\sqrt{2}}{3}\sin^3\theta\cos\theta\cos(3\phi)\right\}. \tag{4}$$

The azimuthal angle ϕ, which defines the magnetization direction in the film plane, is measured with respect to the crystallographic (001) axis of the layer plane for the (100) and the (110) orientations while for the (111) orientation it is measured with respect to the $(\bar{1}10)$ axis. θ is the polar angle.

As regards the interface free energy, E_{inter}, it can be expressed in the lowest symmetry consistent with the symmetry of the respective surface plane as

(100) $$E_{inter} = -k_s\cos^2\theta + k_p\sin^4\theta\cos^2\phi\sin^2\phi \tag{5}$$

(110) $$E_{inter} = -k_s\cos^2\theta + k_p\sin^4\theta\cos^2\phi \tag{6}$$

(111) $$E_{inter} = -k_s\cos^2\theta - k_p\frac{\sqrt{2}}{3}\sin^3\theta\cos\theta\cos(3\phi). \tag{7}$$

In equations (5)–(7), k_s is the out-of-plane anisotropy constant while k_p is the first non-vanishing term of the in-plane interface anisotropy. For $k_s > 0$ the surface normal is an easy axis, while for $k_s < 0$ the film plane is an easy plane of interface anisotropy. Please note that equations (5)–(7) are similarly defined as the projection of the bulk anisotropies on the respective surface plane. The above expressions for the in-plane interface free energy are not unique, in the sense that one can also use other formulations, provided that the crystal in-plane symmetry is correctly taken into account. We would like to emphasize that the expressions for the interface free energy (equations (5)–(7)) need to describe the dependence on the polar angle θ correctly, since due to the precession of the moments an out-of-plane component in the dynamic magnetization exists which interacts with the out-of-plane anisotropy field components H_α and H_β (see below).

Table 1. The first non-vanishing interface anisotropy fields for in-plane-magnetized (100)-, (110)- and (111)-oriented crystal.

	$H_{\alpha'}$	$H_{\beta'}$	$H_{\gamma'}$
(100)	$-\frac{2}{M}(k_s + 2k_p\cos^2\phi\sin^2\phi)$	$\frac{2k_p}{M}(1 - 8\cos^2\phi\sin^2\phi)$	0
(110)	$-\frac{2}{M}(k_s + k_p\cos^2\phi)$	$\frac{2k_p}{M}(2\sin^2\phi - 1)$	0
(111)	$-\frac{2}{M}k_s$	0	$-\frac{k_p}{M}\sqrt{2}\sin(3\phi)$

The volume (H_α, H_β and H_γ) and interface ($H_{\alpha'}$, $H_{\beta'}$ and $H_{\gamma'}$) anisotropy fields for an in-plane-magnetized film ($\theta = 90^\circ$) can be easily obtained from equations (2)–(7) by

applying the following formulae [8]:

$$H_\alpha = \frac{\partial^2}{M\,\partial\theta^2}E_{ani} \qquad H_{\alpha'} = \frac{\partial^2}{M\,\partial\theta^2}E_{inter} \tag{8}$$

$$H_\beta = \frac{\partial^2}{M\,\partial\phi^2}E_{ani} \qquad H_{\beta'} = \frac{\partial^2}{M\,\partial\phi^2}E_{inter} \tag{9}$$

$$H_\gamma = \frac{\partial^2}{M\,\partial\theta\,\partial\phi}E_{ani} \qquad H_{\gamma'} = \frac{\partial^2}{M\,\partial\theta\,\partial\phi}E_{inter} \tag{10}$$

where M is the saturation magnetization. The first non-vanishing interface anisotropy fields for the principal planes of a cubic crystal are reported in table 1.

The following theoretical results are a refinement of those reported in references [1] and [8]. We do not want to describe each step of the calculation and therefore the reader is invited to inspect the equations listed in the appendix. When the anisotropy fields H_γ and $H_{\gamma'}$ are taken into account, the secular equation becomes a sixth-order polynomial equation in the wave-vector component perpendicular to the layers, q_x, rather than a bicubic equation in q_x^2, such as was used in reference [1]. As regards the linear system of eight homogeneous equations, four of them are given by the Rado–Weertman boundary conditions applied at the film interfaces which have to be modified if the (111) crystal orientation is considered, while the remaining four homogeneous equations of the linear system, obtained from the continuity of the parallel component of the field $\boldsymbol{h}$ and the normal component of $\boldsymbol{h}+4\pi\boldsymbol{m}$ at the film interfaces, remain unchanged. We notice that if the values of k_s and k_p are not equal at the two film interfaces, the anisotropy fields entering the Rado–Weertman boundary conditions are different for the two film interfaces ($x = 0$ and $x = -L$). As shown in reference [1], different values of the interface anisotropies on either side of the film result in different spin-wave frequencies for the Damon–Eshbach mode and the exchange modes for $q_\parallel$ and $-q_\parallel$. Therefore, in a BLS experiment the spin-wave frequencies obtained from the Stokes and the anti-Stokes parts of the spectrum may differ in their absolute values. This can be utilized for the separate determination of the interface anisotropy constants of the two interfaces.

3. Comparison between numerical and analytical calculations

In the previous section, we have presented the theoretical model that we use for the numerical calculation of the spin-wave frequencies which are typically observed in a Brillouin light scattering experiment. We note that, when dealing with ultrathin magnetic films where only the Damon–Eshbach spin-wave mode can be detected, the problem of the complexity of the numerical calculation can be overcome by use of a more straightforward analytical procedure. Following the approach proposed by Stamps and Hillebrands [13], one can treat the magnetization as uniform across the magnetic film, and if the product of the film thickness L and the wave vector $q_\parallel$ is small compared to unity, the frequency of the Damon–Eshbach mode for an in-plane-magnetized sample can be expressed as [10]

$$\left(\frac{\omega}{\gamma}\right)^2 = \left[\left(H_0 + H_\alpha + \frac{2}{L}H_{\alpha'} + \frac{2A}{M_s}q_\parallel^2 + 4\pi M f(1 - q_\parallel L/2)\right) \times \left(H_0 + H_\beta + \frac{2}{L}H_{\beta'} + \frac{2A}{M_s}q_\parallel^2 + 2\pi M f q_\parallel L\sin^2\alpha\right) - \left(H_\gamma + \frac{2}{L}H_{\gamma'}\right)^2\right]. \tag{11}$$

The parameter f is the demagnetization factor of ultrathin films, which for $n > 1$ is approximately $f = 1 - 0.2338/n$ with n the number of monolayers [14]. Since the mag-

netization is uniform across the film, the interface torques from the interface anisotropies are converted into volume torques acting on the total film magnetization and the interface anisotropy fields are converted into effective volume anisotropy fields weighed by $2/L$, with the factor of two counting the two interfaces of the film. Rado [15] and Gradmann *et al* [16] give estimates for the range of validity of this assumption. Equation (11) contains both the volume and the interface anisotropy fields and it can be easily applied to Brillouin scattering experiments. We note that the term $H_\gamma + (2/L)H_{\gamma'}$ gives a non-vanishing contribution only for a (111)-oriented crystal.

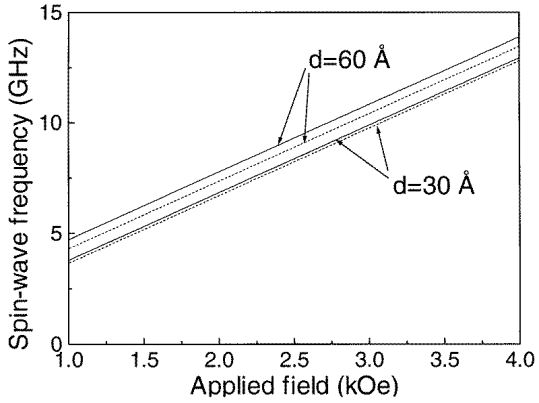

Figure 1. The magnetic field dependence of the Damon–Eshbach mode frequency for two (111)-oriented Ni films, 60 Å and 30 Å thick. The continuous lines are calculated using equation (11) while the dashed lines are calculated by means of the numerical procedure described in the text. For the thicker Ni film $k_p = 0.15$ erg cm^{-2} and $k_s = 0.375$ erg cm^{-2}, while for the thinner film $k_p = 0.07$ erg cm^{-2} and $k_s = 0.210$ erg cm^{-2}. For both Ni films, $K_1 = -5.1 \times 10^4$ erg cm^{-2}.

We would now like to discuss the limit of applicability of equation (11) by means of a comparison to data obtained by using the full numerical procedure. To this end, figure 1 shows the results obtained with the two approaches from the calculation of the spin-wave frequency of (111)-oriented Ni films with thicknesses of 60 Å (the upper two lines) and 30 Å (the lower two lines), respectively. Unless otherwise indicated, we use the following magnetic parameters taken from a fit to the experimental data of a (111)-oriented Ni film 60 Å thick [10]: $\gamma = 1.917 \times 10^7$ Hz Oe^{-1}, $A = 0.73 \times 10^{-6}$ erg cm^{-1}, $4\pi M = 6.03$ kOe. The value of the applied field is always of $H = 1$ kOe, the magnitude of the in-plane wave vector is $q_\parallel = 1.73 \times 10^5$ cm^{-1} and the values of the anisotropy constants are reported in the caption of figure 1. For both films the condition $q_\parallel L \ll 1$ is satisfied. The agreement between the analytical (continuous line) and the numerical (dashed line) calculations is, however, better for the thinner Ni film, $q_\parallel L = 0.052$, where the data almost superimpose, than for the thicker film, $q_\parallel L = 0.104$, where an appreciable frequency difference, which exceeds the Brillouin experimental resolution, is observed. The observed discrepancy of the curves is mainly caused by the approximations made when the terms containing the product $q_\parallel L$ are expanded in power series to first order in the argument $q_\parallel L$ [10]. Using the approximative equation (11) for fitting the experimental data using the anisotropy constant k_s as a fit parameter, one would obtain a value of k_s which is 7% greater than the value obtained by fitting the data using the full numerical procedure. Caution must therefore be exercised when using the analytical approach, even for very low film thicknesses.

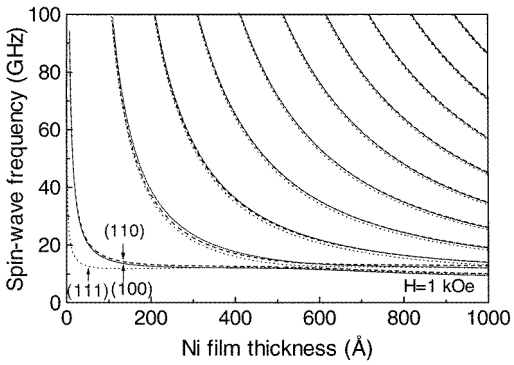

Figure 2. Spin-wave frequencies as functions of the layer thickness for single-crystal Ni (100)-oriented (continuous line), (110)-oriented (dashed line) and (111)-oriented (dotted line) layers. All of the curves are calculated by the full numerical procedure described in the text, taking $\phi = 0$ and assuming the out-of-plane anisotropy constants at the two film interfaces to be equal: $k_s = 0.375$ erg cm^{-2}.

4. Results and discussion

In figure 2 we plot the calculated spin-wave frequencies for Ni (100)-, (110)- and (111)-oriented films as functions of the film thickness. In addition to the surface Damon–Eshbach (DE) mode, a large number of bulk standing modes, characterized by their typical $1/L^2$ behaviour, are visible. While the bulk modes have almost the same thickness dependence, thus being insensitive to the crystal orientation, differences in the DE spin-wave frequency can be observed when the film thickness is reduced below 200 Å. In this condition, interface anisotropy greatly influences the spin-wave frequency, giving rise to an appreciable difference between the principal crystal orientations. These frequency differences are due to the fact that, although the anisotropy constants used to calculate the curves of figure 2 are the same for the three crystal orientations, they enter in different ways in the expression for the interface anisotropy fields (see table 1). In particular, it is well known that the large increase of the frequency of the DE mode, which takes place for Ni film thicknesses lower than 60 Å, is typical of this interface-anisotropy-dominated mode [3]. Another interesting aspect of the spin-wave dispersion curves is the mode repulsion at the branch crossing where the surface and the bulk spin waves interact, interchanging their mode characters.

We now analyse in more detail the spin-wave frequency dispersion as the magnetization direction is varied in the film plane. The main differences between cubic films with different crystallographic orientations will be discussed and information will be gained about the best conditions for determining interface anisotropy constants. For the simulations which follow, the applied field is of 1 kOe and we have throughout kept the volume anisotropy constant fixed to the value [17] $K_1 = 5.1 \times 10^4$ erg cm^{-3} and the out-of-plane anisotropy constant fixed to the value $k_s = 0.375$ erg cm^{-2}. Figure 3 shows the spin-wave dispersion of the Damon–Eshbach mode as a function of the angle ϕ for the principal planes of a Ni film that is 200 Å thick. All of the curves are calculated by means of the full numerical procedure described in section 2, with the in-plane interface anisotropy constant k_p set to zero. Therefore the directional dependence of the spin-wave frequency is only caused by the magnetocrystalline bulk anisotropy in the simulations. Maxima in the spin-wave frequencies indicate easy directions of the magnetization. For the (111)-oriented film, the frequency shows a sixfold periodicity which reflects the in-plane layer symmetry,

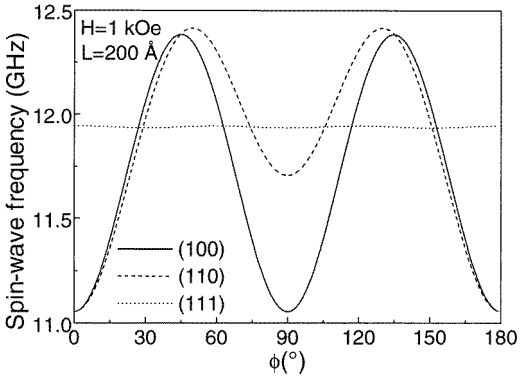

Figure 3. Spin-wave frequencies for the principal planes of a cubic crystal as functions of the angle ϕ for an applied magnetic field of 1.0 kOe. The in-plane anisotropy is set to zero at both film interfaces.

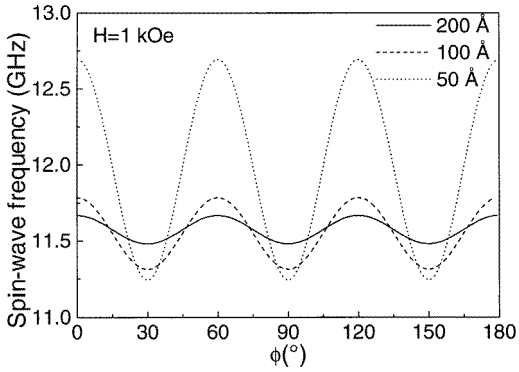

Figure 4. Spin-wave frequencies for (111)-oriented cubic crystal as functions of the angle ϕ for film thicknesses of 200 Å, 100 Å and 50 Å.

and the amplitude of the frequency oscillation is greatly reduced with respect to those relating to the (100)- and the (110)-oriented films. For these last two orientations, the fourfold and twofold angular periodicities result from the respective symmetries of the bulk anisotropy fields [8]. Our calculations indicate that the experimental determination of the in-plane anisotropy constants from the spin-wave frequency dispersion is very difficult for thick Ni(111) films since the frequency dispersion with the in-plane angle is comparable with or lower than the typical Brillouin scattering resolution ($\simeq$0.3 GHz). This type of measurement becomes more feasible in the case of ultrathin films since the interface anisotropy constant k_p, converted into an effective volume anisotropy field, yields a large contribution to the angular dispersion of the spin-wave frequency. To illustrate this aspect, the calculated angular dispersion of the spin-wave frequency for a (111)-oriented Ni film that is 200 Å thick is compared in figure 4 with that of Ni films of lower thicknesses (100 Å and 50 Å). The curves are calculated assuming the interface anisotropy constants $k_p = 0.15$ erg cm^{-2} and $k_s = 0.375$ erg cm^{-2}. The peak-to-peak frequency amplitude, which essentially depends on k_p, increases from about 0.2 GHz, for the thick films, to approximately 1.4 GHz, for the Ni film that is 50 Å thick. This is within the range of sensitivity of a typical BLS experiment. Results of the analysis of the directional

variation of the spin-wave frequency of Ni films 25 Å, 30 Å and 60 Å thick are reported elsewhere [10].

5. Conclusions

We have studied the dispersion of dipolar (Damon–Eshbach modes) and exchange-dominated spin waves for in-plane-magnetized thin and ultrathin cubic films with (111) crystal orientation. A quantitative comparison between the results of the complete numerical approach and those obtained using a simplified analytical expression valid in the ultrathin-film limit has shown that even for a Ni film as thin as 60 Å a suitable correction of the out-of-plane anisotropy constant k_s has to be made in order to achieve a reasonable consistency of the data. The results obtained for the (111) orientation have been compared with those relating to the other principal planes of a cubic crystal. It has been shown that while the frequency variation versus the angle ϕ in thick films is rather small, this variation increases in ultrathin films because of the greater contribution given by the in-plane anisotropy energy which is converted into an effective volume anisotropy. We believe that the results presented in this paper will stimulate further BLS investigations of the magnetic anisotropy on the (111) planes of ultrathin films and multilayers.

Acknowledgments

GG would like to thank the University of Kaiserslautern for hospitality during a three-month visit. He also acknowledges financial support (a PhD grant) from the University of Camerino, Italy.

Appendix

Referring to the equations contained in reference [1] as equations (An) where n indicates the equation number, we list the refinements of those expressions which enter in the spin-wave frequency calculation for a cubic crystal with (111) orientation:

$$Mh_y + \left(\frac{\mathrm{i}\omega}{\gamma} - H_\gamma\right)m_x - \left[H + H_\beta + 2\frac{A}{M}q^2\right]m_y = 0 \tag{A13}$$

$$-Mh_x + \left[H + H_\alpha + 2\frac{A}{M}q^2\right]m_x + \left(\frac{\mathrm{i}\omega}{\gamma} + H_\gamma\right)m_y = 0 \tag{A14}$$

$$\frac{\mathrm{d}E_{ani}}{\mathrm{d}\alpha_x} = H_\alpha m_x + H_\gamma m_y \tag{A16}$$

$$\frac{\mathrm{d}E_{ani}}{\mathrm{d}\alpha_y} = H_\gamma m_x + H_\beta m_y. \tag{A17}$$

On introducing the effective fields H_a and H_b which are defined in reference [8], the secular equation assumes the following form:

$$\left[\frac{\omega^2}{\gamma^2} + H_\gamma^2 - H_a H_b\right]q^2 - 4\pi M[H_b q_x^2 + H_a q_y^2 - 2H_\gamma q_x q_y] = 0. \tag{A22}$$

It can be converted into a polynomial equation:

$$\sum_{i=0}^{6} a_i q_x^i = 0$$

with the following coefficients:

$$a_0 = q_\parallel^6 + \frac{M}{2A}(2H + H_\alpha + H_\beta + 4\pi M)q_\parallel^4 + \left(\frac{M}{2A}\right)^2\left[(H + H_\beta)(H + H_\alpha + 4\pi M) - H_\gamma^2 - 8\pi A q_z^2 - \left(\frac{\omega^2}{\gamma^2}\right)\right]q_\parallel^2 + 4\pi M\left(\frac{M}{2A}\right)^2[(H_\alpha - H_\beta)q_\parallel^2 - (H + H_\alpha)q_z^2]$$

$$a_1 = -8\pi M H_\gamma q_y\left(\frac{M}{2A}\right)^2$$

$$a_2 = \left\{3q_\parallel^4 + 2q_\parallel^2\left(\frac{M}{2A}\right)(2H + H_\alpha + H_\beta + 4\pi M) + \left(\frac{M}{2A}\right)^2\left[(H + H_\beta)(H + H_\alpha + 4\pi M) - H_\gamma^2 - 8\pi A q_z^2 - \frac{\omega^2}{\gamma^2}\right]\right\}$$

$$a_3 = 0$$

$$a_4 = \left[3q_\parallel^2 + \left(\frac{M}{2A}\right)(2H + H_\alpha + H_\beta + 4\pi M)\right]$$

$$a_5 = 0$$

$$a_6 = 1.$$

Also,

$$u_i = \frac{M}{D}\left[H_b - \frac{q_y}{q_{xi}}\left(\frac{\mathrm{i}\omega}{\gamma} + H_\gamma\right)\right] \tag{A26}$$

$$v_i = \frac{M}{D}\left[H_a - \frac{q_y}{q_{xi}}\left(\frac{\mathrm{i}\omega}{\gamma} - H_\gamma\right)\right] \tag{A27}$$

where

$$D = H_a H_b - H_\gamma^2 - \left(\frac{\omega^2}{\gamma^2}\right)$$

and A is the exchange stiffness constant.

The Rado–Weertman boundary conditions calculated at the two film surfaces become

$$\sum_{i=1}^{6}[(MH_{\alpha'} - 2\mathrm{i}Aq_{xi})u_i + MH_{\gamma'}v_i]h_{xi} = 0 \tag{A37a}$$

$$\sum_{i=1}^{6}[(MH_{\alpha'} + 2\mathrm{i}Aq_{xi})u_i + MH_{\gamma'}u_i]h_{xi}\mathrm{e}^{\mathrm{i}q_{xi}L} = 0 \tag{A37b}$$

$$\sum_{i=1}^{6}[MH_{\gamma'}u_i + (MH_{\beta'} - 2\mathrm{i}Aq_{xi})v_i]h_{xi} = 0 \tag{A38a}$$

$$\sum_{i=1}^{6}[MH_{\gamma'}u_i + (MH_{\beta'} + 2\mathrm{i}Aq_{xi})v_i]h_{xi}\mathrm{e}^{\mathrm{i}q_{xi}L} = 0. \tag{A38b}$$

All of the quantities which appear in the previous equations reduce to those reported in reference [1] when $H_\gamma = 0$ and $H_{\gamma'} = 0$. In the original paper there was a misprint in

equation (34), whose correct form is

$$\sum_{i=1}^{6}(1+4\pi u_i)h_{xi}\mathrm{e}^{-\mathrm{i}q_{xi}d_n} - h^e_{x1}\mathrm{e}^{-q_\parallel d_n} - h^e_{x2}\mathrm{e}^{q_\parallel d_n} = 0. \tag{A34}$$

References

[1] Hillebrands B 1990 *Phys. Rev.* B **41** 530
[2] Rupp G, Wettling W, Smith R S and Jantz W 1984 *J. Magn. Magn. Mater.* **45** 404
[3] Hillebrands B, Baugmart P and Guntherodt G 1987 *Phys. Rev.* B **36** 2450
[4] Krams P, Lauks F, Stamps R L, Hillebrands B and Guntherodt G 1992 *Phys. Rev. Lett.* **69** 3674
[5] Hichen R J, Eley D E P, Gester M, Gray S J, Daboo C, Ives A J R and Bland J A C 1995 *J. Magn. Magn. Mater.* **145** 278
[6] Subramanian S, Liu X, Stamps R L, Sooryakumar R and Prinz G A 1995 *Phys. Rev.* B **52** 10 194
[7] Liu X, Steiner M, Sooryakumar R, Prinz G A, Farrow R F C and Harp G 1996 *Phys. Rev.* B **53** 12 166
[8] Hillebrands B 1998 *Light Scattering in Solids VII (Springer Topics in Applied Physics)* ed M Cardona and G Guntherodt (Berlin: Springer) at press
[9] Rezende S M, Moura J A S, de Aguiar F M and Schreiner W H 1994 *Phys. Rev.* B **49** 15 105
[10] Gubbiotti G, Carlotti G, Socino G, D'Orazio F, Lucari F, Bernardini R and De Crescenzi M 1997 *Phys. Rev.* B **56** 11 073
[11] Bozorth R M 1993 *Ferromagnetism* (New York: IEEE Press) p 579
[12] This expression is directly obtained from the definition of the magnetocrystalline energy of a cubic crystal, equation (1), on introducing the direction cosines of the magnetization: $\alpha_x = (1/\sqrt{3})[\cos\theta + \sqrt{2}\sin\theta\cos\phi]$, $\alpha_y = (1/\sqrt{3})[\cos\theta + \sqrt{2}\sin\theta\cos(\phi - (2/3)\pi)]$, $\alpha_z = (1/\sqrt{3})[\cos\theta + \sqrt{2}\sin\theta\cos(\phi - (4/3)\pi)]$, in a rotated coordinate system with the z'-axis along the (111) direction.
[13] Stamps R L and Hillebrands B 1991 *Phys. Rev.* B **44** 12 417
[14] Heinrich B, Celinski Z, Cochran J F, Arrott A S and Myrtle K 1990 *Phys. Rev.* B **44** 530
[15] Rado G T 1987 *J. Appl. Phys.* **61** 4262
[16] Gradmann U, Korecki J and Waller G 1986 *Appl. Phys.* A **39** 101
[17] Crangle J 1977 *The Magnetic Properties of Matter* (London: Edward Arnold) p 112